



OSL dating of a Pleistocene maar: Birket Ram, the Golan heights

Uri Shaanan ^{a,*}, Naomi Porat ^b, Oded Navon ^a, Ram Weinberger ^b, Andrew Calvert ^c, Yishai Weinstein ^d

^a Institute of Earth Sciences, The Hebrew University, Jerusalem 91904, Israel

^b Geological Survey of Israel, 30 Malkhe Israel St., Jerusalem 95501, Israel

^c Volcano Science Center, U.S. Geological Survey, 345 Middlefield Road, Menlo Park, CA 94025, USA

^d Department of Geography and Environment, Bar-Ilan University, Ramat-Gan 52900, Israel

ARTICLE INFO

Article history:

Received 27 February 2010

Accepted 12 June 2010

Available online 23 June 2010

Keywords:

maar
geochronology
OSL dating
⁴⁰Ar/³⁹Ar
Golan

ABSTRACT

Direct dating of maars and their phreatomagmatic deposits is difficult due to the dominance of lithic (host rock) fragments and glassy particles of the juvenile magma. In this paper we demonstrate that optically stimulated luminescence (OSL) dating can be successfully used for age determination of phreatomagmatic deposits. We studied the tuff deposit of Birket Ram, a basanitic maar located at the northern edge of the Golan heights on the western Arabian plate. The maar is underlain by a thick section of Pleistocene basalts, and currently hosts a small lake. It is filled by approximately 90 m of lacustrine sediments with radiocarbon ages extrapolated to 108 ka at the base. OSL was applied to quartz grains extracted from tuffs and paleosols in order to set the time frame of the phreatomagmatism at the site. A maximum age constraint of 179 ± 13 ka was determined for a paleosol that underlies the maar ejecta. Quartz grains from two layers in the tuff section yielded a direct age of 129 ± 6 ka for the phreatomagmatic eruption. A younger age of 104 ± 7 ka, which was determined for a tuff layer underlying a basaltic flow, was attributed to thermal resetting during the lava emplacement. This was confirmed by an ⁴⁰Ar/³⁹Ar age of 101 ± 3 ka determined on the overlying basalt. The internal consistency of the OSL ages and the agreement with the ⁴⁰Ar/³⁹Ar age determination as well as with previous estimates demonstrates the potential of OSL for maar dating.

© 2010 Elsevier B.V. All rights reserved.

1. Introduction

A maar is a phreatomagmatic monogenetic vent that penetrates the surrounding host rock (Lorenz, 1986, 2007). Phreatomagmatic eruptions usually last for a short time, on the order of days or weeks, as was documented in recent events of maar formation (Lorenz, 2007). Pleistocene maars are mostly dated using indirect methods, including radiocarbon in lake sediments (Ehrlich and Singer, 1976; Brauer et al., 2000; Benedetti et al., 2008), ⁴⁰Ar/³⁹Ar of tephra layers interbedded in the maar lake sediments (Roger et al., 2000; Pastre et al., 2007), as well as U-series dating of related basalts (Aka et al., 2008). Direct dating of the phreatomagmatic deposits is uncommon, because the ejecta is mainly composed of host-rock fragments which usually retain their original age during the low temperature eruption.

Occasionally, when the juvenile material in the tuff is crystalline, it can be dated by the ⁴⁰Ar/³⁹Ar method (McDougall and Harrison, 1999; Roger et al., 1999, 2000; Giaccio et al., 2009). Optically Stimulated Luminescence (OSL) is a dating method that is usually applied to sediments of Upper Pleistocene to Holocene ages (Wintle, 2008) and is based on electrons trapped in imperfections of quartz or alkali-feldspar

lattices (Aitken, 1998). Electron accumulation in the lattice traps is a function of in-situ radiation and of time. Controlled laboratory thermal or optical stimulation of the crystal releases the trapped electrons to produce a luminescence signal. In nature, these electrons can be released by heat or by sunlight, resulting in resetting of the signal. Measuring the dose that the material had absorbed, which created the luminescence signal, compared to the field dose it was exposed to and its lattice specific absorption potential, enables calculating the time since crystal formation or since the last reset (Aitken, 1998).

Quartz grains are uncommon in mafic volcanic provinces but they may be present as lithic clasts in phreatomagmatic deposits or in paleosols that underlie or cover the tuff. This paper demonstrates that OSL can be a powerful dating tool in these difficult-to-date volcanic structures.

2. Geological setting

The Cenozoic volcanic activity in western Arabia is characterized as intra-plate, alkaline magmatism (mostly alkali basalts and basanites; Shaw et al., 2003; Weinstein et al., 2006). Harrat Ash Shaam is the largest volcanic field in this province (Fig. 1A). The maar of Birket Ram is located in the northern Golan, at the northwestern edge of this field, where the volcanic sequence covers Jurassic and Cretaceous sedimentary rocks at

* Corresponding author.

E-mail address: uri.shaanan@mail.huji.ac.il (U. Shaanan).

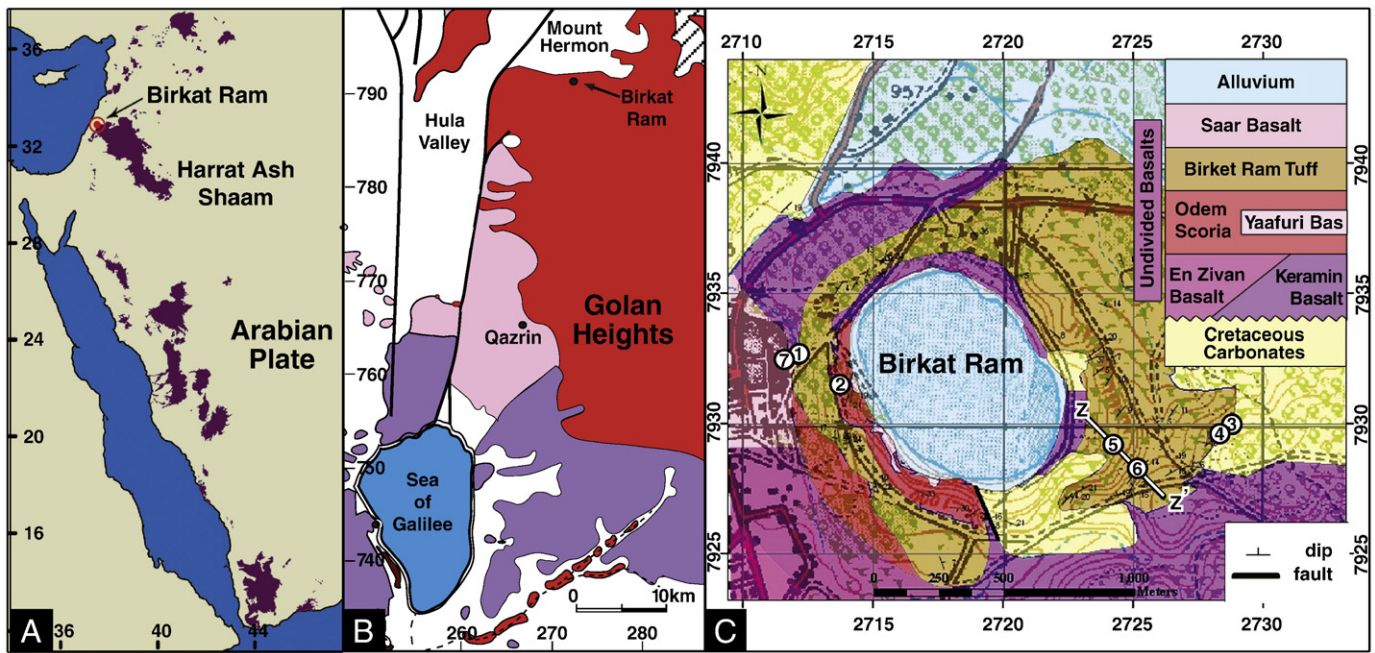


Fig. 1. A. Cenozoic volcanic fields of the western Arabian plate and location of Birkat Ram maar in the Harrat Ash Shaam volcanic field. B. Map of the volcanic units in the Golan (the northwestern part of Harrat Ash Shaam). Purple and pink areas marks Lower and Upper Pliocene volcanic units, respectively and the red area indicates Pleistocene volcanism. Non-volcanic rock units are in white (after Weinstein et al., 2006). C. Geological map of the Birkat Ram maar (Shaanan, 2009). The numbers mark the locations of the sampling sites.

the foot of Mount Hermon. Structurally, the maar is located along a N10W lineament of scoria cones (Mor, 1987), sub-parallel to the Red Sea Rift and to other lineaments in Harrat Ash Shaam (Garfunkel, 1989). It is the only maar in this area and one of the two known phreatomagmatic sites in the Golan heights (Weinstein and Weinberger, 2006; Weinstein, 2007).

The maar is elliptical, 1000 by 1200 m in diameter, which is a medium-sized maar according to the classification of Gevrek and Kazanci (2000). Most of its surface is covered by a shallow lake, up to 15 m deep (Fig. 2).

The unique setting of Birkat Ram caught the eyes of people in ancient times, and Josephus Flavius (1st century AD) described it as a lake-filled volcanic crater (Flavius J., AD 75 [translation by Williamson G. A., published in, 1959]). A borehole drilled in the center of the maar indicates that the lake is underlain by at least 90 m of lacustrine sediments, underlain in turn by phreatomagmatic ejecta (Tahal drilling logs, Shaanan, 2009).

The local stratigraphy includes Upper Cretaceous (Cenomanian and Turonian) carbonates (Mor, 1987), unconformably covered by a



Fig. 2. Birkat Ram maar viewed from the southeast. Sampling sites are marked by dots and arrows. The arrows are for sites that do not actually show in the picture due to the topography.

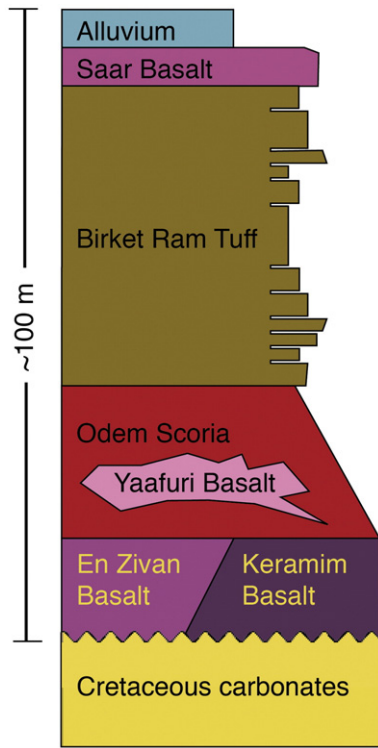


Fig. 3. Schematic stratigraphy of the rock units at Birket Ram.

thick section (>200 m) of Pleistocene basalts, which fill a local depression (Shaanan, 2009). The effusive activity was followed by a strombolian eruption, which built a scoria cone at the southwestern part of the maar (Fig. 1C). Both the Upper Cretaceous sedimentary rocks and the Pleistocene volcanics are covered by the phreatomagmatic deposits of the maar. West of the maar, the Saar Basalt covers the tuff and marks the termination of the volcanic activity in this area (Fig. 3).

The maar was never directly dated, but some age constraints exist. The Keramim Basalt, which directly underlies the tuff in several places around the maar (Figs. 1C and 3), yielded an $^{40}\text{Ar}/^{39}\text{Ar}$ age of 223 ± 3 ka (Feraud et al., 1983; Goren-Inbar, 1985). A lacustrine sediment from a depth of 36 m beneath the maar lake floor yielded a radiocarbon age of 29 ± 4 ka. This was extrapolated back to 108 ka at the base of the lake-filling sediments (Ehrlich and Singer, 1976) (Fig. 4). Mor (1993) determined a K–Ar age of 140 ± 80 ka for the Saar Basalt, which covers the tuff (Fig. 3). Altogether, these ages

roughly define a time window of 110–220 ka for the phreatomagmatic eruption of Birket Ram.

3. Birket Ram Tuff

The phreatomagmatic deposits of Birket Ram (Birket Ram Tuff, hereafter BRT) include tuff, lapilli-tuff and large accidental fragments, which were deposited from surges and fallout. BRT is exposed over an area of 1.15 km² around the maar. The thickness of the tuff reaches a maximum of 45 m at the southeastern rim of the maar (section z–z', Fig. 1C).

BRT is mainly composed of rock fragments of the local stratigraphic section, while juvenile material (palagonitic glass) forms less than 50%. Most of the rock fragments (80%) are from the volcanic section and the rest are carbonates from the underlying sedimentary rocks. The BRT also contains quartz grains, which were derived either from the surface (from soils with quartz of aeolian origin) or from the underlying Lower Cretaceous sandstones (Fig. 5A and B). These quartz grains were used for the OSL dating.

4. Sampling and methods

The luminescence dating method determines the age of the last event of exposure to light or of thermal heating of mineral grains such as quartz and feldspar (Aitken, 1998). In Birket Ram we used quartz grains found in the tuff and paleosols. Five outcrops of paleosols and tuffs were chosen for OSL dating. Sample BRU-1 is from a tuff section northwest of the maar. It was sampled 0.25 m below the base of the overlying Saar Basalt, (Figs. 1C and 2). Samples BRU-2 and BRU-3 were collected from paleosols located, respectively, at the western and eastern flanks of the maar (see Figs. 1C and 2), and BRU-4 was collected from a tuff layer 1 m above BRU-3. Samples BRU-5 and BRU-6 are from the southeastern inner rim of the maar. BRU-5 was sampled 11 m above the exposed base of the tuff section, and BRU-6 18 meters higher. The samples were collected by augering into vertical outcrops or, when the sediments were too consolidated, by removing blocks, which were later cleaned in the laboratory.

Gamma and cosmic dose rates were measured in the field using a portable gamma scintillator. Water contents in the sediment samples were measured immediately after sampling. Alpha and beta dose rates were calculated from the concentrations of the radionuclides U, Th, and K in the sediment, measured by ICP-MS. Quartz grains, 74–250 μm in size, were separated under subdued orange lighting and purified from the bulk sediment using standard laboratory procedures (Porat, 2007). Luminescence measurements were carried out on Risø DA-12 or DA-20 TL/OSL readers. The equivalent doses (De) were determined using the single aliquot regenerative dose (SAR) protocol (Murray and

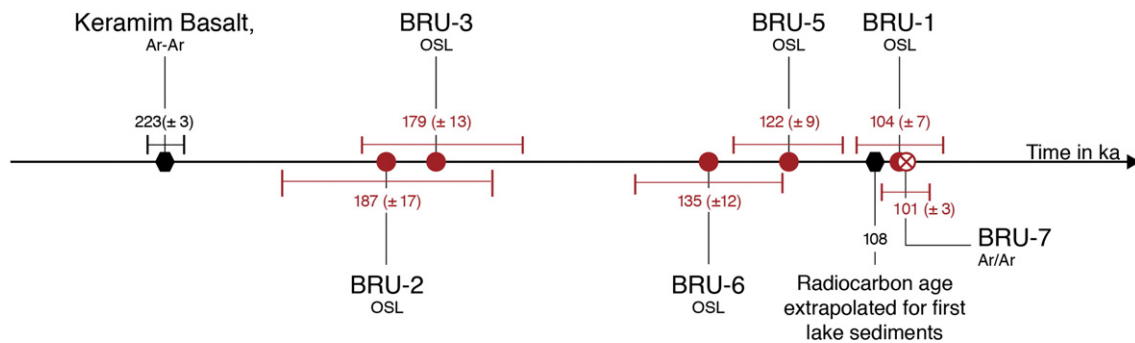


Fig. 4. Time line showing the geochronology of the Birket Ram deposits based on radiocarbon, $^{40}\text{Ar}/^{39}\text{Ar}$, and OSL ages. The OSL ages are marked by (red) solid circles and the $^{40}\text{Ar}/^{39}\text{Ar}$ age by a (red) crossed circle. Black hexagons mark earlier geochronological ages (Ehrlich and Singer, 1976; Feraud et al., 1983; Goren-Inbar, 1985).

Wintle, 2000) and the obtained OSL signal. For each sample, twelve to nineteen 2-mm aliquots were measured and the most representative De and associated errors were calculated using the central age model (Galbraith et al., 1999). Only seven aliquots were measured for BRU-6, due to the small number of quartz grains extracted from this sample.

Sample BRU-7 was taken from the Saar Basalt northwest of the maar (Figs. 1C and 2) and it was dated by the $^{40}\text{Ar}/^{39}\text{Ar}$ incremental heating technique. Dense, clean groundmass was separated, irradiated at the USGS TRIGA reactor facility, and analyzed in the USGS-Menlo Park geochronology laboratory following techniques described in Calvert and Lanphere (2006). Neutron flux was monitored using a 27.87 Ma TCR-2 sanidine.

5. OSL results

The OSL ages range from 104 ± 7 ka to 187 ± 17 ka (Table 1). The signal is dominated by the fast component (Fig. 6A and B), recycling ratios are mostly within 7% of unity (Fig. 6C), and the infrared depletion ratios are within 5% of unity. This suggests that the SAR protocol is appropriate for the measured samples (Wintle and Murray, 2006). Dose response curves were fitted with a saturation + exponential fit. The De values do not vary as a function of preheat temperature between 200–260 °C (Fig. 6D), implying that the OSL signal measured is stable over this temperature range. The De values of some of the samples (BRU-5 and BRU-6) show a rather large scatter (Fig. 6E), probably due to non-uniform heating or exposure to sunlight of the quartz grains during the eruption.

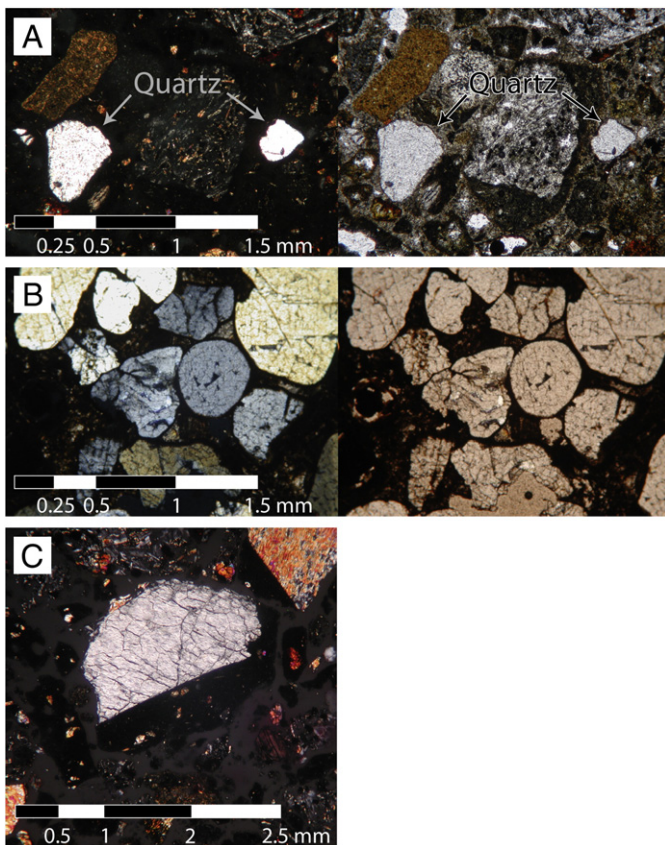


Fig. 5. A. Photomicrographs of a tuff sample (Birket Ram Tuff), containing quartz grains of Lower Cretaceous sandstone (left – cross polarized light, right – plane polarized). B. Photomicrographs of Lower Cretaceous sandstone from the flanks of Mount Hermon (~1 km away from the maar) with grains exhibiting signs of deformation, fractured fragments, joints and Fe-coating. Similar features can be seen in quartz grains found in the tuff (left – cross polarized light, right – plane polarized). C. Photomicrograph (cross polarized light) of a tuff sample with a fragment of Keramim Basalt (in the tuff) carries a 2 mm quartz grain.

The two paleosols BRU-2 and BRU-3 (Table 1 and Figs. 1C, 2 and 4), which underlie the tuff, yielded similar ages of 187 ± 17 ka and 179 ± 13 ka, respectively, providing a maximum age for the phreatomagmatic eruption. Of the four tuff samples, BRU-4 yielded an old age, incompatible with the other ages (Table 1). Most likely this sample was not fully exposed to heat or light and the OSL signal was not completely reset at the time of the eruption. The samples from the southeastern rim of the maar (Fig. 1C) yielded ages that agree within error (see Fig. 4), although BRU-6, which is 18 m higher in the stratigraphy, turned out to be older than BRU-5 (135 ± 12 ka and 122 ± 9 ka, respectively). The limited number of aliquots measured for BRU-6 renders its age less representative. Sample BRU-1 yielded a significantly younger age (104 ± 7 ka). This sample is from a tuff layer directly overlain by the Saar Basalt, and as discussed below, its younger age is attributed to thermal resetting during the emplacement of the basalt (Figs. 1C, 2, 3 and 4).

6. $^{40}\text{Ar}/^{39}\text{Ar}$ results

The Saar Basalt yielded a 101 ± 3 ka (1σ) plateau age, 100 ± 3 ka total gas age, and 100 ± 8 ka isochron age using 100% of the ^{39}Ar released (Fig. 7). All incremental heating steps are concordant and the $^{40}\text{Ar}/^{36}\text{Ar}$ intercept on the isochron suggests all contaminant argon is atmospheric in composition.

7. Discussion

We constrained the age of the phreatomagmatic eruption that formed the Birket Ram maar by OSL dating of accidental quartz grains in the tuff and paleosols. The composition of the phreatomagmatic deposits and all neighboring and underlying volcanic rocks are alkali basalts to basanites. Thus, the quartz grains in the tuff should be allocthonous, brought either by surface transport processes or by magmatic transport from subsurface sedimentary rock strata. Lower Cretaceous quartzaceous sandstones are exposed on the nearby slopes of Mount Hermon (Mor, 1987), and found as well in the subsurface of Birket Ram, at depths of at least 800 m (extrapolated from the exposed Upper Cretaceous rocks at the maar rims; Fig. 1C).

The quartz grains found in the paleosols are similar to the grains in modern local soils and are, most likely, aeolian (Ganor and Foner, 1996). The fine fraction ($< 100 \mu\text{m}$) was transported as dust from distant southern sources (Arabia or the Sahara) through regional atmospheric circulation (Ganor and Foner, 1996; Kubilay et al., 2000). On the other hand, the coarser quartz grains (up to a diameter of 2 mm), which show deformation features (undulatory extinction, fractured faces and joints) and Fe-coatings (Fig. 5B; Shaanan, 2009), resemble the quartz in the nearby outcrops of the Lower Cretaceous sandstone.

The origin of the quartz grains in the tuff deposits is less clear. One possibility is that they were entrapped by the magma during its ascent through subsurface sandstone layers, before encountering the surface water. This is supported by the occurrence of similar quartz grains in the Keramim Basalt that underlies the tuff (Fig. 5A and C). In this model, quartz grains were reset by the heat of the magma. The incomplete resetting of BRU-4 could have resulted from magmatic transport of large sandstone fragments, in which temperatures at the core of the fragment did not exceed the required 400 °C for more than a minute (Aitken, 1985).

An alternative explanation for the occurrence of the quartz grains in the tuff is that it could have been 'sampled' during the phreatomagmatic eruption (after encountering the water and fragmentation) from the underlying sandstone layers or from subaerial alluvium or soils. However, this is less favorable, since the quartz grains are equally distributed along the tuff section, while conventional theories of maar formation describe initial shallow explosions and a diatreme deepening with time (Lorenz, 1986). Nevertheless, we

Table 1
Details of the OSL measurements.

Sample no.	Field γ ($\mu\text{Gy/a}$)	Moisture (%)	K (%)	U (ppm)	Th (ppm)	Ext. α ($\mu\text{Gy/a}$)	Ext. β ($\mu\text{Gy/a}$)	Dose rate ($\mu\text{Gy/a}$)	Aliquots used	De (Gy)	Age (ka)
BRU-1	855	14	0.54	2.2	10.3	9	775	1640 \pm 93	12/12	171 \pm 7	104 \pm 7
BRU-2	826	18	0.73	1.7	7.2	6	737	1569 \pm 88	13/14	294 \pm 22	187 \pm 17
BRU-3	721	24	0.52	3.9	4.4	8	750	1478 \pm 85	18/19	265 \pm 11	179 \pm 13
BRU-4	630	17	0.29	2.0	9.0	8	560	1198 \pm 71	11/13	327 \pm 21	273 \pm 24
BRU-5	844	13	1.00	1.4	6.0	5	879	1729 \pm 96	15/15	212 \pm 10	122 \pm 9
BRU-6	859	7	1.16	1.6	5.0	6	1044	1909 \pm 96	6/7	257 \pm 20	135 \pm 12
BRU-5 and 6									21/22		129 \pm 6

Quartz samples, grain size 74–250 μm . All samples were etched by concentrated HF for 40 min. Field gamma was measured in-situ and includes a cosmic dose component. This gamma dose was later attenuated for moisture contents. 'Aliquots used' is the number of aliquots used for the De calculations out of those measured. The most representative $\text{De} \pm 1\text{ s}$ for each sample was calculated using the central age model (Galbraith et al., 1999). A combined age for BRU-5 and BRU-6 was calculated from the ages (and not De values) of the individual aliquots, thus accounting for the different dose rates.

cannot exclude this model, since in karstic and fractured rocks such as the local limestones and basalts (Kattan, 1997; Shulman et al., 2004; Rimmer and Salingar, 2006), fragmentation may occur two to three times deeper than in that predicted by the conventional theory, which was defined for lithostatic pressure. Last, the quartz grains also could have been sampled from the surface (soils) during the phreatomagmatic eruption.

Taken all together, the quartz in the tuff could have been reset either thermally (entrapment by magma or during the explosion) or by exposure to sunlight slightly before or during the eruption. Another possible mechanism that could have reset the OSL signal is the hydrostatic pressure, as was suggested for clastic dikes near the Dead Sea, Israel (Porat et al., 2007). A similar mechanism, perhaps

augmented by heating, was suggested for the Ulmen Maar and Pulvermaar in the West Eifel Volcanic Field, Germany (Zöller et al., 2009). Resetting due to pressure at low temperature could not be reproduced experimentally (Zöller et al., 2009), and this mechanism awaits further clarification.

7.1. The age of the phreatomagmatic eruption

The quartz in the paleosols underlying the tuff was reset by exposure to sunlight before the onset of the eruption; thus, the youngest paleosol age provides a maximum age of $179 \pm 13\text{ ka}$ for the phreatomagmatic eruption (sample BRU-3). The quartz in the tuff should provide the age of the eruption itself. Tuff samples BRU-5 and

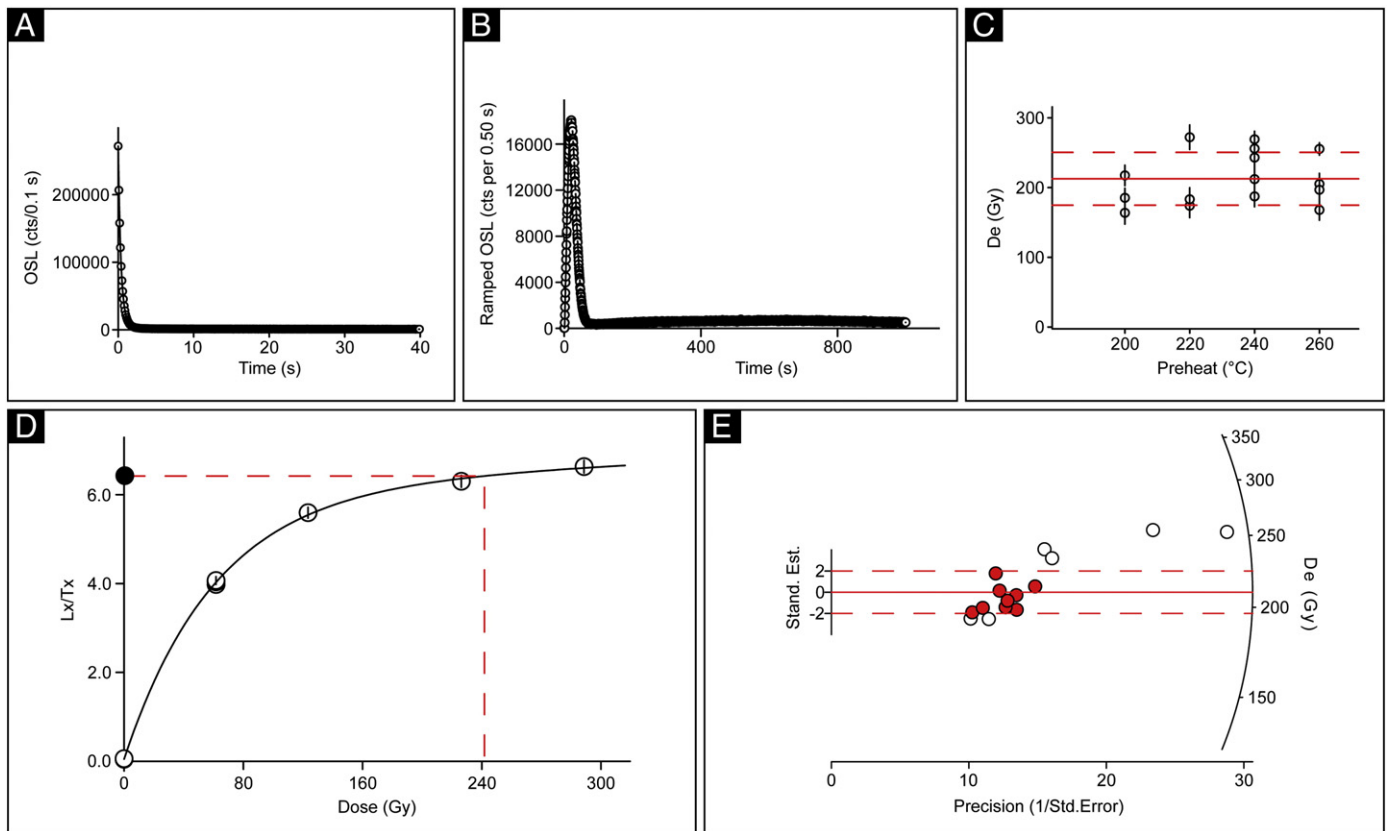


Fig. 6. Luminescence dating analyses for sample BRU-5. A. Natural OSL signal for an aliquot. B. Ramped OSL signal, whereby the intensity of the stimulation source (blue LED) is increased from 0 to 100% over 1000 s. Most of the OSL signal is emitted within 5% of LED intensity, implying that the signal is dominated by the fast component. C. Dose response curve for an aliquot. The signal grows as a function of the given laboratory beta dose until the natural signal can be regenerated. The second dose point from the left was repeated 3 times and the recycling ratios are ~ 0.98 . D. Preheat plateau showing that the De values do not change as a function of preheat temperature, hence the measured signal is stable over a temperature range of 200–260 $^{\circ}\text{C}$. E. Radial plot showing the De values plotted as a function of the reciprocal relative error.

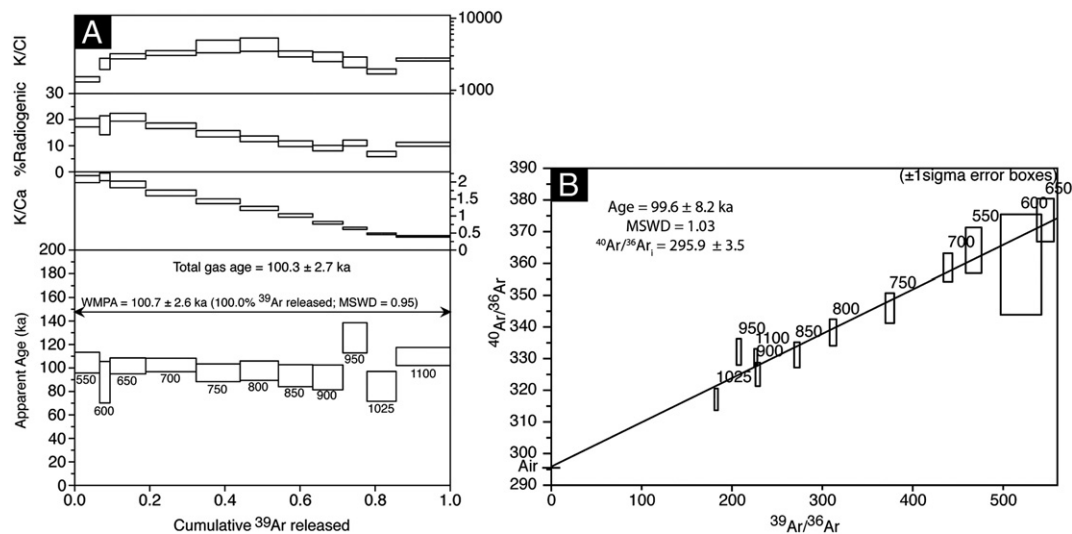


Fig. 7. $^{40}\text{Ar}/^{39}\text{Ar}$ geochronology for sample BRU-7. A. Age spectrum, K/Ca and K/Cl ratios and radiogenic yield during incremental heating of 143 mg groundmass concentrate. Errors shown are ± 1 sigma. B. Isotope correlation (isochron) diagram.

BRU-6 from the southeastern section yielded ages of 122 ± 9 ka and 135 ± 12 ka, respectively, younger than the underlying paleosols (Fig. 4). The absence of paleosols within the tuff section and the commonly accepted short life time of phreatomagmatic eruptions (e.g., Lorenz, 2007) suggest that the whole tuff section, including these two samples, was deposited within a short time. To better constrain the timing of the eruption, the measurements from the two samples were combined (Table 1), providing an average age of 129 ± 6 ka for the phreatomagmatic eruption.

Another tuff sample (BRU-1) from the northwestern flank of the maar yielded a significantly younger age of 104 ± 7 ka. Since this sample is located only 0.25 m below the contact with the Saar Basalt, we suggest that the luminescence signal of the quartz grains in this sample was thermally reset by heat emanating from the overlying lava. Similar cases, where quartz-bearing sediments were thermally reset by lava flows, were reported and dated using thermoluminescence from Mount Gambier, Australia (Robertson et al., 1996), and from the Massif Central, France, (Bassinet et al., 2006). The $^{40}\text{Ar}/^{39}\text{Ar}$ age of the overlying Saar Basalt (101 ± 3 ka) is in excellent agreement with the above-mentioned OSL age (Fig. 4), confirming our interpretation of that OSL date as a thermal reset age.

The OSL ages presented here are in good agreement with the earlier, non-direct geochronological studies (Ehrlich and Singer, 1976; Feraud et al., 1983; Goren-Inbar, 1985; Mor, 1993). New $^{40}\text{Ar}/^{39}\text{Ar}$ ages of basalts and scoriae defined two main phases of activity in the northern Golan (Inbar and Gilichinsky, 2009; Weinstein et al., unpublished data). The early phase occurred between 600 and 750 ka and the later phase between 100 to 150 ka. The OSL ages of Birket Ram fit well within the time span of the late volcanic phase, which interestingly includes the only two phreatomagmatic sites known from the Golan heights.

Being aware of the difficulties in applying other dating methods to phreatomagmatic deposits, and considering the common occurrence of quartz in soils and sediments, we suggest that the OSL method should be considered as a major dating tool in maar structures.

8. Conclusions

- The quartz in the tuff of Birket Ram enables defining the time of the phreatomagmatic eruption that produced the maar.
- The quartz in the paleosols underlying the tuff in Birket Ram was optically reset and provides an OSL maximum age of ~ 180 ka for the phreatomagmatic eruption.

- The quartz grains in the tuff yielded an age of 129 ± 6 ka for the phreatomagmatic eruption.
- The 104 ± 7 ka age of quartz grains in a tuff layer that underlies a flow of the Saar Basalt represents thermal resetting by the flow. This is confirmed by a $^{40}\text{Ar}/^{39}\text{Ar}$ age of 101 ± 3 ka determined on the overlying basalt.
- The ages of the phreatomagmatic eruption (129 ± 6 ka) and the Saar Basalt (101 ± 3 ka) fit well within the time span of the late volcanic phase in the northern Golan (100–150 ka).
- OSL dating of quartz or feldspar-bearing tephra may be applied to other Pleistocene phreatomagmatic features.

Acknowledgments

This research is based on part of the first author M.Sc. thesis at the Institute of Earth Sciences, The Hebrew University, Jerusalem. The work was supported by the Israeli Ministry of National Infrastructures, grant nos. ES-30-2005 and ES-47-2006.

References

- Aitken, M.J., 1985. Thermoluminescence Dating. Academic Press, London, p. 359.
- Aitken, M.J., 1998. An Introduction to Optical Dating. Oxford University Press, Oxford, p. 267.
- Aka, T.F., Yokoyama, T., Kusakabe, M., Nakamura, E., Tanyileke, G., Ateba, B., Ngako, V., Nnange, J., Hell, J., 2008. U-series dating of Lake Nyos maar basalts, Cameroon (West Africa): implications for potential hazards on the Lake Nyos dam. *J. Volcanol. Geoth. Res.* 176, 212–224.
- Bassinet, C., Mercier, N., Miallier, D., Pilleyre, T., Sanzelle, S., Valladas, H., 2006. Thermoluminescence of heated quartz grains: intercomparisons between SAR and multiple-aliquot additive dose techniques. *Radiat. Meas.* 41, 803–808.
- Benedetti, A.A., Funiello, R., Giordano, G., Diano, G., Caprilli, E., Paterne, M., 2008. Volcanology, history and myths of the Lake Albano maar (Coli Albani volcano, Italy). *J. Volcanol. Geoth. Res.* 176, 387–406.
- Brauer, A., Endres, C., Zolitschka, B., Negendank, F.W.J., 2000. AMS radiocarbon and varve chronology from the annually laminated sediment record of lake Meerfelder maar. Germany. *Radiocarbon* 42, 355–368.
- Calvert, A.T., Lanphere, M.A., 2006. Argon geochronology of Kilauea's early submarine history. *J. Volcanol. Geoth. Res.* 151, 1–18.
- Ehrlich, A., Singer, A., 1976. Late Pleistocene diatom succession in a sediment core from Birket Ram, Golan heights. *Isr. J. Earth Sci.* 25, 138–151.
- Feraud, G., York, D., Hall, C.M., Goren, N., Schwarcz, H.P., 1983. $^{40}\text{Ar}/^{39}\text{Ar}$ age limit for an Acheulian site in Israel. *Nature* 304, 263–265.
- Flavius, J., AD 75. The Jewish War (Translated from Greek by Williamson, G. A. 1959). Penguin Books, England. Pp. 511.
- Galbraith, R.F., Roberts, R.G., Laslett, G.M., Olley, J.M., 1999. Optical dating of single and multiple grains of quartz from jinnium rock shelter, northern Australia: part I, experimental design and statistical models. *Archaeometry* 41 (2), 339–364.
- Ganor, E., Foner, H.A., 1996. The mineralogical and chemical properties and the behaviour of aeolian Saharan dust over Israel. In: Guerzoni, S., Chester, R. (Eds.),

- The Impact of Desert Dust Across the Mediterranean. Kluwer Academic Publishers, The Netherlands, pp. 163–172.
- Garfunkel, Z., 1989. Tectonic setting of Phanerozoic magmatism in Israel. *Isr. J. Earth Sci.* 38, 51–74.
- Gevrek, A.I., Kazanci, N., 2000. A Pleistocene, pyroclastic-poor maar from central Anatolia, Turkey: influence of a local fault on a phreatomagmatic eruption. *J. Volcanol. Geoth. Res.* 95, 309–317.
- Giaccio, B., Marra, F., Hajdas, I., Karner, D.B., Renne, P.R., Sposato, A., 2009. $^{40}\text{Ar}/^{39}\text{Ar}$ and ^{14}C geochronology of the Albano maar deposits: implications for defining the age and eruptive style of the most recent explosive activity at Colli Albani Volcanic District, Central Italy. *J. Volcanol. Geoth. Res.* 185, 203–213.
- Goren-Inbar, N., 1985. The lithic assemblage of the Berekhat Ram Acheulian site, Golan Heights. *Paleorient* 11, 7–28.
- Inbar, M., Gilichinsky, M., 2009. New Ar/Ar dates from lava flows and cinder cones in the Golan Heights—some geomorphic implications. *Isr. Geol. Soc. Annu. Meet.* 68.
- Kattan, Z., 1997. Environmental isotope study of the major karst springs in Damascus limestone aquifer systems: case of the Figeih and Barada springs. *J. Hydrol.* 193, 161–182.
- Kubilay, N., Nickovic, S., Moulin, C., Dulac, F., 2000. An illustration of the transport and deposition of mineral dust onto the eastern Mediterranean. *Atmos. Environ.* 34, 1293–1303.
- Lorenz, V., 1986. On the growth of maars and diatremes and its relevance to the formation of tuff-rings. *B. Volcanol.* 48, 265–274.
- Lorenz, V., 2007. Syn- and post-eruptive hazards of maar-diatreme volcanoes. *J. Volcanol. Geoth. Res.* 159, 285–312.
- McDougall, I., Harrison, T.M., 1999. *Geochronology and Thermochronology by the $^{40}\text{Ar}/^{39}\text{Ar}$ Method*. Oxford University Press, p. 269.
- Mor, D., 1987. The geological map of Israel, Har Odem. Geological Survey of Israel, sheet 2-II, scale 1:50,000, sheet 1.
- Mor, D., 1993. A time-table for the Levant Volcanic Province, according to K–Ar dating in the Golan Heights. *Isr. J. Afr. Earth Sci.* 16, 223–234.
- Murray, A.S., Wintle, A.G., 2000. Luminescence dating of quartz using an improved single-aliquot regenerative-dose protocol. *Radiat. Meas.* 32, 57–73.
- Pastre, J.F., Gauthier, A., Nomade, S., Ort, P., Andrieu, A., Goupille, F., Guillou, H., Kunesch, S., Scaillet, S., Renne, P.R., 2007. The Alleret maar (Massif Central, France): a new lacustrine sequence of the early Middle Pleistocene in western Europe. *C. R. Geosci.* 339, 987–997.
- Porat, N., 2007. Analytical procedures in the luminescence dating laboratory. Technical Report TR-GSI/2/2007. Geol. Surv. Isr. 42 (in Hebrew).
- Porat, N., Levi, T., Weinberger, R., 2007. Possible resetting of quartz OSL signal during earthquakes — evidence from injection dikes in Late Pleistocene sediments, Dead Sea basin, Israel. *Quat. Geochronol.* 2 (1–4), 272–277.
- Rimmer, A., Salinger, Y., 2006. Modelling precipitation-streamflow processes in karst basin: the case of the Jordan River sources, Israel. *J. Hydrol.* 331, 524–542.
- Robertson, G.B., Prescott, J.R., Hutton, J.T., 1996. Thermoluminescence dating of volcanic activity at Mount Gambier, South Australia. *Trans. R. Soc. S. Aust.* 120, 7–12.
- Roger, S., Coulon, C., Thouveny, N., Féraud, G., Van Velzen, A., Fauquette, S., Cochemé, J.J., Prévot, M., Verosub, K.L., 2000. $^{40}\text{Ar}/^{39}\text{Ar}$ dating of a tephra layer in the Pliocene Senèze maar lacustrine sequence (French Massif Central): constraint on the age of the Réunion–Matuyama transition and implications on paleoenvironmental archives. *Earth Planet. Sci. Lett.* 183, 431–440.
- Roger, S., Féraud, G., De Beaulieu, J.-L., Thouveny, N., Coulon, C., Cochemé, J.J., Andrieu, V., Williams, T., 1999. $^{40}\text{Ar}/^{39}\text{Ar}$ dating on tephra of the Velay maars (France): implications for the Late Pleistocene proxy-climatic record. *Earth Planet. Sci. Lett.* 170, 287–299.
- Shaanan, U., 2009. Birket Ram maar. Report GSI/13/2009. Geol. Surv. Isr. 73 (in Hebrew, with English abstr.).
- Shaw, E.J., Baker, A.J., Menzies, A.M., Thirlwall, F.M., Ibrahim, M.K., 2003. Petrogenesis of the largest intraplate volcanic field on the Arabian plate (Jordan): a mixed lithosphere–asthenosphere source activated by lithospheric extension. *J. Petrol.* 44 (9).
- Shulman, H., Reshef, M., Ben-Avraham, Z., 2004. The structure of the Golan Heights and its tectonic linkage to the Dead Sea Transform and the Palmyrides folding. *Isr. J. Earth Sci.* 53, 225–237.
- Weinsein, Y., 2007. A transition from Strombolian to phreatomagmatic activity induced by a lava flow damming water in a valley. *J. Volcanol. Geoth. Res.* 159, 167–284.
- Weinstein, Y., Navon, O., Altherr, R., Stein, M., 2006. The role of lithospheric mantle heterogeneity in the generation of Plio-Pleistocene alkali basaltic suites from NW Harrat Ash Shaam (Israel). *J. Petrol.* 47 (5), 1017–1050.
- Weinstein, Y., Weinberger, R., 2006. The geology and volcanological history of Mount Avital. *Isr. J. Earth Sci.* 55, 237–255.
- Wintle, A.G., 2008. Luminescence dating: where it has been and where it is going. *Boreas* 37, 471–482.
- Wintle, A.G., Murray, A.S., 2006. A review of quartz optically stimulated luminescence characteristics and their relevance in single-aliquot regeneration dating protocols. *Radiat. Meas.* 41, 369–391.
- Zöller, L., Blanchard, H., McCammon, C., 2009. Can temperature assisted hydrostatic pressure reset the ambient TL of rocks? — a note on the TL of partially heated country rock from volcanic eruptions. *Anc. TL* 27 (1), 15–22.